U.P.B. Sci. Bull., Series B, Vol. 79, Iss. 2, 2017 ISSN 1454-2331

INFLUENCE OF UNIDIRECTIONAL SOLIDIFICATION IN BRIDGMAN FURNACE ON THE MECHANICAL BEHAVIOR OF A CAST ALUMINUM ALLOY

Iuliana STAN [1], Constantin Stelian STAN [2]

Crystallization and unidirectional solidification in aluminum alloys was investigated using a three zone furnace with the solidifying melt placed in a mobile crucible moving vertically upwards. The solidification conditions were modified based upon a set of four melting – solidification – cooling diagrams. Overheating and cooling temperatures, as well as the solidification – cooling speeds have been varied. Six samples were selected for investigation in Bridgman furnace at 973 K (700°C), 1023 K (750°C) and 1073 K (800°C) temperatures. These samples were investigated for mechanical properties. The approval test had the same values for the compression strength, regardless of the analysis position. For the other samples, it was noticed that the compression strength was influenced by the increase of the overheating temperature and cooling rate. The highest compressive strength was obtained for the 1073 K (800°C) overheating temperature and was approximately 37% higher than the approval test. Comparing the values of compressive strength for the same sample, but considering the delimitation zone, it was remarked a significant difference, between 10 and 20%.

Keywords: Bridgman, unidirectional solidification, aluminum alloys, structure, mechanical properties.

1. Introduction

In the Bridgman process [1, 2] the heat transfer depends on the thermal conductivity, as well as the mould thickness. The ability to release the heat through radiation from the outer surface influences the heat absorption process and the thermal profile in the mould face, as well as the heat transfer between the mould inner surface and the injected sample that lead to higher temperatures in these areas. The Bridgman method or unidirectional solidification method is a method for production big components (like vanes, blades, etc) that can also be optimized for small components (e.g. engine components, etc). In general, the lower cooling rates during solidification process [3] lead to a coarse microstructure and present a great tendency for formation of casting defects.

[1] Engineer, Materials Science and Engineering Faculty, University POLITEHNICA of Bucharest, Romania, e-mail: iuliana_stefania@yahoo.com;

[2] Associate Professor, Materials Science and Engineering Faculty, University POLITEHNICA of Bucharest, Romania, e-mail: constantin.stan@upb.ro.

In the last years, there was an increased interest for aluminum alloys studies [4-6] generally speaking and especially on advanced casting methods that are based on higher thermal gradients during solidification process. These gradients can reduce or eliminate the problems caused by the cast products sizes and also by the low cooling rates in conventional Bridgman process [7, 8]. In particular, the method is efficient for reducing casting defects and for obtaining of fine microstructure in big components. In a comparison between Bridgman method and liquid-metal-cooled (LMC) method have been measured the cooling rates and was found that the cooling rates in LMC method were up to 7.5 times higher than those of Bridgman process, with a reduction of 2 times of the space between primary dendritic arms [9, 10]. Elliott and Pollack [10] showed that the LMC thermal aspects are more complex than those of Bridgman process due to the suddenly thermal transition in the furnace from the hot zone to the cold one, increasing the amount of extracted heat. The thermal conditions during the solidification process determines the casts microstructure, that influences directly the materials mechanical properties and control the grain structure, microporosity, carbide distribution and defects that can be reduce under a large temperature gradient. Thermal data from the relevant zones of the castings combined with the computerized calculation models can give a more complete view of solidification process and also allow the prediction of defects and post-solidification properties.

LMC process was investigated for the first time in 1970, in laboratory, but it was not widely used, therefore has not been an analysis of the process benefits. Many elements of the LMC thermal process are similar to those that occur during Bridgman unidirectional solidification. Increasing the calculation speed by process computer simulations allowed process simulations for simplified geometries in asymmetrical configurations. Unfortunately, current models are not capable to realize a rigorous simulation of casting conditions through unidirectional solidification with complex three-dimensional geometries, in a reasonable time, due to the complexity of the thermal processes. The castings geometry and non-axial thermal extraction proved to have a significant impact on the space between the dendrite branches and on the growth crystallographic orientation. Unidirectional solidification modeling of LMC process [8, 9] has been limited to a simulation on an axi-symmetric one-dimensional bar, being simplified the conditions assessed to the heat flow at the mould-cooling fluid interface. None of these models did not took into account the thermal conditions between the cooling liquid and the metal itself during the simulation, due to the process complexity. The most detailed analysis was conducted of Kermanpur and his collaborators [11] using a simplified condition: time – temperature – heat dependent by the heat transfer. Elliott and Pollock [10, 12] developed both Bridgman and LMC DS model using ProCAST simulation package. Data and process parameters for casting experiments have been used to interfere with the limit shaping conditions and to verify the model predictions. LMC solidification analysis described by them leads further to the possibility of LMC process modeling. This model more fully takes into account variations in the fluid flow and variations in temperature together with the cooling fluid bath that are really critical parameters of LMC process. Bridgman and LMC models are also used to investigate contribution and sensitivity of each stage of the thermal transfer process.

Due to the temperature difference between the liquid and the solid phase, as well as the solubility difference between the two phases, it can be established in the dendritic solidification structure a redistribution of the liquid phase. Crystallization and unidirectional solidification may be easily obtained using a furnace with several zones, inside of which a crucible moves containing the melt that is in the solidifying process. These kinds of furnaces are called Bridgman furnaces (Fig. 1) and are designed so that the crystal growth can take place at a lower temperature gradient and in which different kinds of alloys and materials can be melted and solidified [3].

The control system maintains the desired thermal profile during the crystal growth. The final quality of the crystal depends on several physical phenomena, such as: thermal transfer processes, hydrodynamic processes, chemical processes or thermo-mechanical interaction.

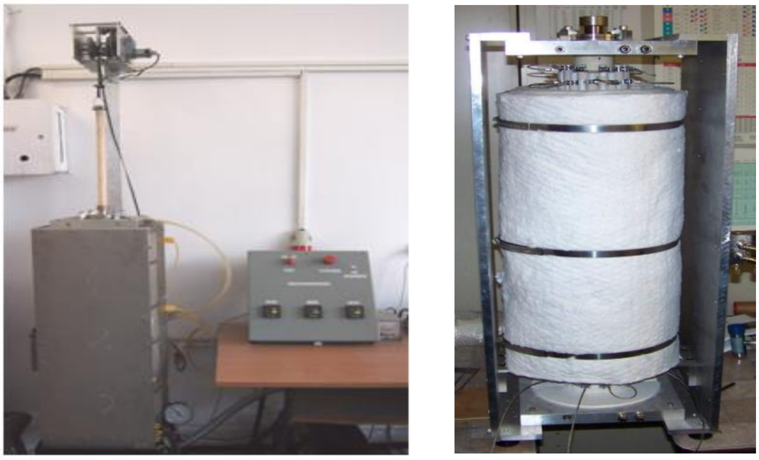

(a) **(b)**

Fig. 1. (a) the Bridgman equipment; (b) the Bridgman furnace.

The differences between these two methods are:

- heat absorption by the cooling plate (LMC) becomes very quickly ineffective as the solidification front moves away from the cooling plate due to relatively low thermal conductivity;

- comparing Bridgman and LMC casting methods was observed that the cooling rates in LMC process were up to 7.5 times higher than in Bridgman process;
- in LMC method the area of the primary dendrite branches have been reduced by 2 times;
- thermal aspects of LMC process are more complex than those of the Bridgman process due to sudden thermal transition, from the heat zone to the cold one increasing the amount of heat extracted in the oven;
- in the case of Bridgman solidification, the heat disposal from the mold surface takes place by radiation, whereas in LMC method heat transfer takes place by conduction and convection, that gives high efficiency to the LMC process due to the productive release of heat;
- in the Bridgman process, the metal mold is moved from the heated zone into the cold one;
- in the Bridgman model, the process is neither limited by the extraction of heat, nor by the advance of the solidification front of the cast sample.

Based on these aspects, the influence of unidirectional solidification on the properties of an aluminum alloy will be analyzed using a Bridgman furnace, considering the fact that aluminum alloys are some of the most widely used materials today, spanning the entire range of industries [13, 14].

2. Materials and Methods

The experimental program used for aluminum investigation assumed the melting - solidification - cooling from which have been selected six samples [15]. The chemical composition of aluminum is presented in Table 1. Bridgman furnace, type 1200, used for experiments is shown in Fig. 2.

Table 1

The chemical composition for the aluminum alloy used in the experiments

Element	***Al***	***Si***	***Mg***	***Cu***	***Others***
Wt.%	98.0	0.7	0.22	0.16	balance

The samples were obtained by melting - solidification - cooling of the aluminum following the diagrams that are shown in Fig. 3 (a – d). Thus, in Fig. 3 (a) is presented the melting - solidification - cooling diagram for the first sample (approval test) obtained by melting the aluminum in an alumina crucible and by raising the temperature from 293 K (20°C) up to 973 K (700°C), with a heating rate of 283 K/min (10°C/min), maintaining the melt at this temperature for 64 minutes and cooling it with a rate of 278 K/min (5°C/min) up to ambient temperature.

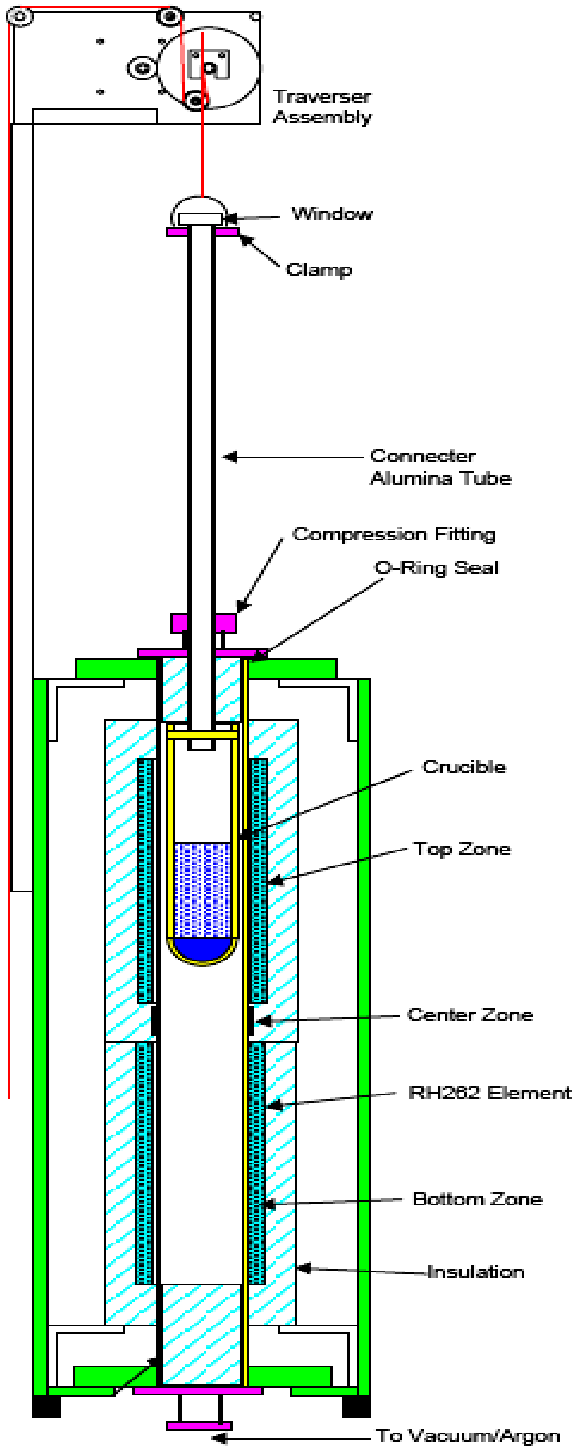

Fig. 2. The Bridgman furnace, type 1200

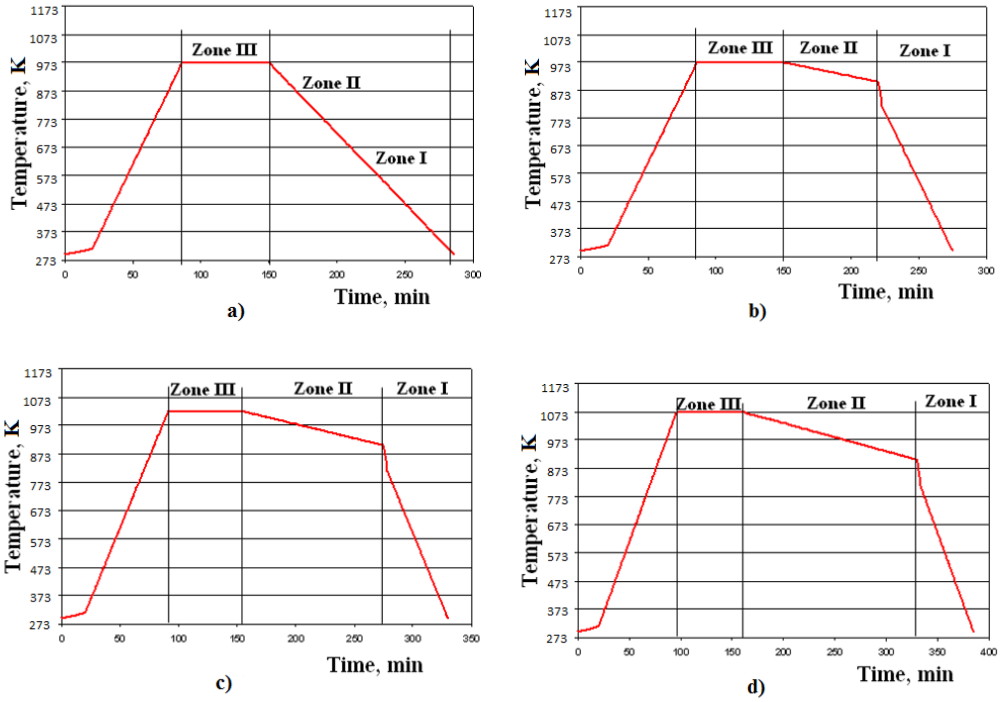

Fig. 3. Melting – solidification – cooling diagrams of aluminum samples in Bridgman furnace:
a) approval test; b) sample 1, T_{max} = 973 K (700°C), cooling rate 273 K/min (1°C/min);
c) sample 2 and sample 3, T_{max} = 1023 K (750°C), cooling rate 273 K/min (1°C/min);
d) sample 4 and sample 5, T_{max} = 1073 K (800°C), cooling rate 273 K/min (1°C/min).

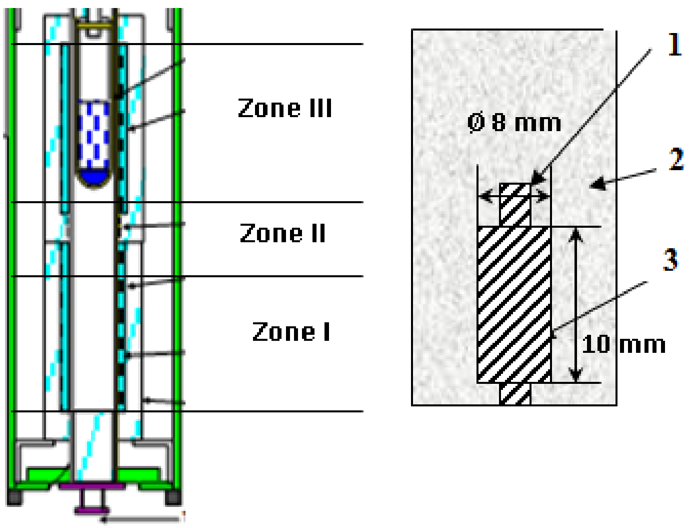

Fig. 4. Samples for compression tests: 1 - mechanical testing sample (zone II);
2 - solidified aluminum sample in the Bridgman furnace;
3 - mechanical testing sample (zone I).

The next sample (sample 1 from Fig. 3b) has been obtained by melting the aluminum and raising the temperature up to 973 K (700°C), maintaining the melt at this temperature for 64 minutes, cooling from 973 K (700°C) to 903 K (630°C) with a speed of 273 K/min (1°C/min), then cooling from 903 K (630°C) to 813 K (540°C) with a rate of 303 K/min (30°C/min), followed by a cooling with 283 K/min (10°C/min) up to ambient temperature. For the other two sets of samples (samples 2, 3, 4 and 5, Fig. 3c and 3d), the same cooling rates have been maintained, with the exception that the maximum temperatures was 1023 K (750°C), respectively 1073 K (800°C), and the maintaining time also 64 minutes. After the samples melting – solidification – cooling, 6 specimens with the dimensions of Ø75 x 150 mm were obtained, which were cut and prepared for mechanical testing. Thus, 12 samples with the dimensions of Ø8 x 10 mm were obtained (for compression tests), as it is shown in Fig. 4.

3. Results and Discussions

In Table 2 are presented the results obtained for the samples investigated at different melting – solidification – cooling rates, after the compression tests, based on the stress-strain curves, acquired with an INSTRON 3382 equipment. The compression tests have been realized up to a nominal strain of 35%. Thus, the compression strength value (σ_{max}) that was determined corresponds to a deformation ε = 35% for all the tests (at compression, σ_{max} being the maximum compresive strength). In Fig. 5, the stress-strain diagrams are presented.

Table 2

Mechanical characteristics obtained after compression tests

Mechanical charact. / ***Sample***	***Temperature,* K (°C)**	***Tensile-compression strength* σ_{max} [MPa]**	***Yield strength* $\sigma_{0,2}$ [MPa]**
Approval test	973 (700)	247	59
1. I-st zone	973 (700)	281	74
1. II-nd zone		247	63
2. I-st zone	1023 (750)	300	83
2. II-nd zone		275	78
3. I-st zone	1023 (750)	309	98
3. II-nd zone		268	85
4. I-st zone	1073 (800)	335	108
4. II-nd zone		281	83
5. I-st zone	1073 (800)	339	118
5. II-nd zone		293	87

σ_{max} – compression strength, corresponding to a deformation of $\varepsilon = 35\%$ (for all samples);
$\sigma_{0,2}$ – yield strength.

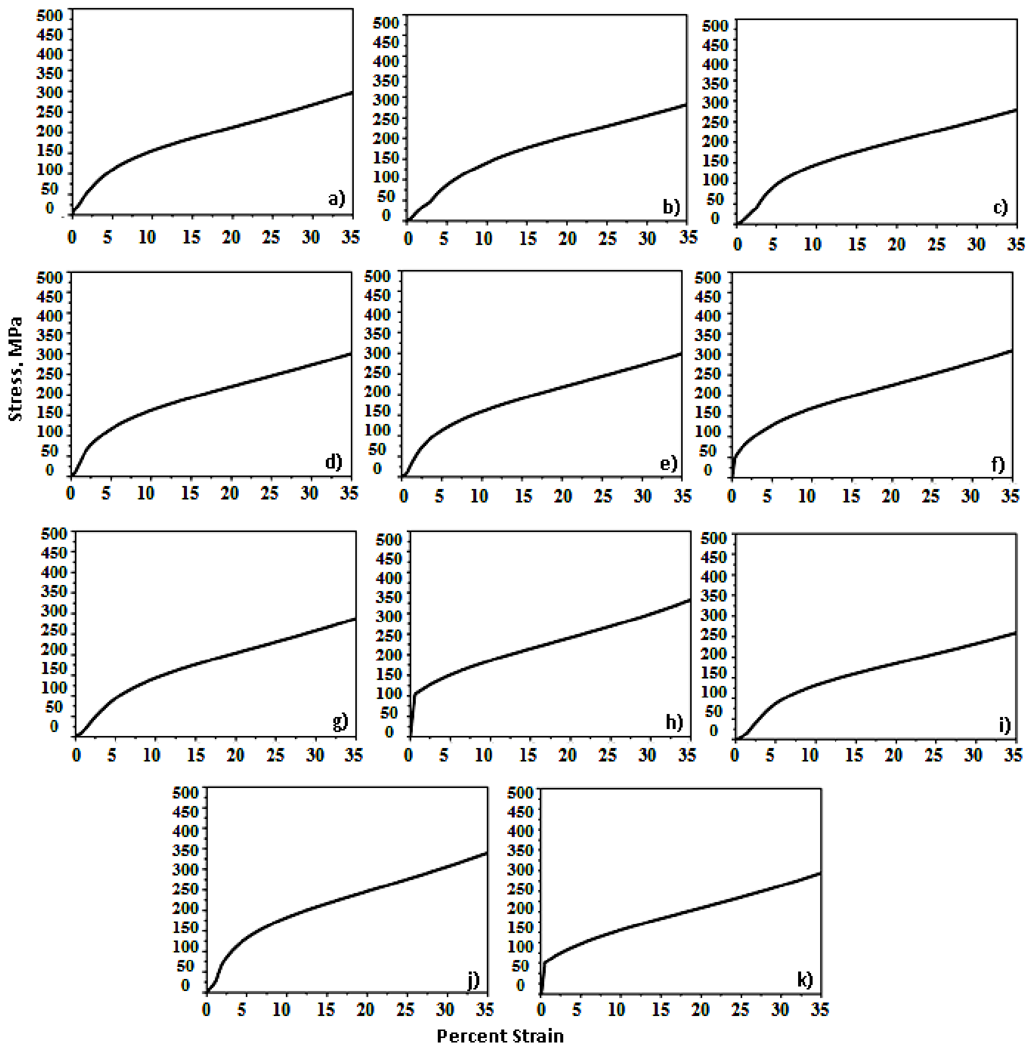

Fig. 5. Stress-strain diagrams obtained with the Instron 3382 equipment: a - approval test; b - sample 1 in I-st zone; c - sample 1 in II-nd zone; d - sample 2 in I-st zone; e - sample 2 in II-nd zone; f - sample 3 in I-st zone; g - sample 3 in II-nd zone; h - sample 4 in I-st zone; i - sample 4 in II-nd zone; j - sample 5 in I-st zone; k - sample 5 in II-nd zone.

For the melted – solidified – cooled samples in Bridgman furnace the following conclusions are obtained analyzing the results presented in Table 2 and Figs. 6 and 7, in which the compression strength and yield strength values are displayed, determined with the help of stress-strain diagrams. Thus, in case of compression strength the minimum value was recorded in the approval test without directional solidification (247 MPa), the structure being the same in both zones. It can be observed that the compression strength has the highest value for the overheating temperature T = 1073 K (800°C) respectively 339 MPa for the samples solidified in I-st zone and 293 MPa for samples solidified in II-nd zone. The compression strength was influenced by the increase of overheating temperature, as well as by the cooling rate.

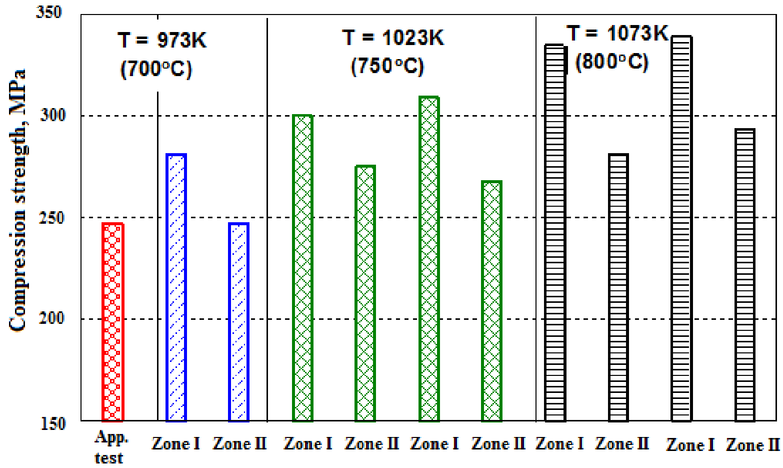

Fig. 6. The influence of cooling rate on compression strength

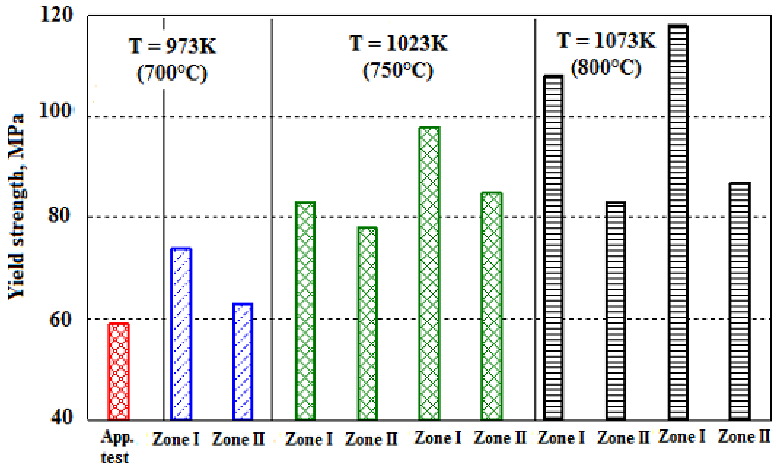

Fig. 7. The influence of cooling rate on yield strength

Comparing the values obtained for each sample in the two investigation zones, it can be noted that:

a. For sample 1 - overheated up to 973 K (700°C) temperature - the compression strength for the sample solidified in I-st zone was with 34 MPa higher than the compression strength of the sample solidified II-nd zone (corresponding to the diagram 3 b), i.e. with 13.7% higher. The average compression resistance for this sample was 287.5 MPa, higher with 17 MPa compared with the approval test, i.e. by 6.88% higher.

b. For samples 2 and 3 - overheated up to temperature 1023 K (750°C) - the compression strength of the solidified sample in I-st zone was with 25 MPa, respectively 41 MPa higher than the compression strength in the solidified sample in II-nd zone (according to the diagram shown in Fig. 3c). The average compression resistance was 287.5 MPa for sample 2 and 288.5 MPa for sample 3. It was higher with 40 MPa, respectively with 41.5 MPa than the approval test, i.e. about 16% higher. The average compression strength for samples 2 and 3, solidified under the same conditions, was 288 MPa and was higher with 16.6% than the approval test.

c. For samples 4 and 5 – overheated up to 1073 K (800°C) temperature - the compression strength for the solidified sample in I-st zone was 54 MPa, respectively 46 MPa, higher than the compression strength in the solidified sample in II-nd zone (according to the diagram of Fig. 3 d), i.e. about 16% higher than the approval test. The average compression strength for samples 4 and 5 were 308 MPa and 316 MPa, higher with 61 MPa, respectively 69 MPa, than the approval test. The average compression strength for samples 4 and 5 was 312 MPa, higher with 26% than the same property determined on the approval test.

Analysing the yield strength, it was noticed that the conventional yield strength had 118 MPa the maximum value, for the sample overheated at 1073 K (800°C) (sample 5) and the minimum value 59 MPa, for the approval test. The differences between the zones from which the samples have been chosen are between 11 MPa (in case of sample 1) and 31 MPa (for sample 5), the average values for each sample between the two zones being: 9.5 MPa for sample 1, 21.5 MPa for sample 2, 32.5 MPa for sample 3, 36.5 MPa for sample 4, 43.5 MPa for sample 5. The average value calculated on each obtained sample, under the same conditions, recorded values with 16% (for sample 1), 45% (for sample 2 and 3), respectively 68% (for sample 4 and 5) higher than the approval test.

If each sample obtained under the same conditions of overheating temperature and cooling rate is considered, one can say that:

a. For sample 1 – overheated up to 973 K (700°C) temperature - the cooling from 973 K (700°C) to 903 K (630°C) was done with a cooling rate of 273 K/min (1°C/min), then from 903 K (630°C) to 813 K (540°C) with a cooling rate of 303 K/min (30°C/min), followed by a cooling rate of 283 K/min (10°C/min) up to ambient temperature**.** The difference between the conventional yield strength in the I-st and in the II-nd zone was 11 MPa. The average value was 68.5 MPa and it was with 10% higher than the approval test. The difference between the maximum value recorded in the I-st zone and the approval test was 15 MPa, which means 25% higher than the approval test.

b. For samples 2 and 3 - overheated up to 1023 K (750°C) temperature - the cooling from 1023 K (750°C) to 903 K (630°C) was done with a cooling rate of 273 K/min (1°C/min), then from 903 K (630°C) to 813 K (540°C) with 303

K/min (30°C/min), followed by a cooling rate of 283 K/min (10°C/min) till the ambient temperature. The difference between the conventional yield strength in the I-st and in the II-nd zone was 5 MPa in case of sample 2 and 13 MPa for sample 3. The average value of the two zones was 80.5 MPa for the sample 2 and 91.5 MPa for the sample 3. The difference between the maximum value recorded in the I-st zone and the approval test was 39 MPa, and was noticed for sample 3, or it was with 66% higher than the approval test. The average value for the two samples was 86 MPa and 27 MPa greater than the approval test (with 45% higher).

c. For samples 4 and 5 – overheated up to 1073 K (800°C) temperature – the cooling from 1073 K (800°C) to 903 K (630°C) was conducted with a cooling rate of 273 K/min (1°C/min), then from 903 K (630°C) to 813 K (540°C) with a cooling rate of 303 K/min (30°C/min), followed by a cooling rate of 283 K/min (10°C/min). The difference between the yield strength in the I-st and in the II-nd zone was 25 MPa in case of sample 4 and respectively 31 MPa for sample 5. The average value of the two zones was 95.5 MPa, respectively 102.5 MPa for samples 4 and 5. The difference between the maximum recorded value in the I-st zone and the approval test was 59 MPa and was recorded for sample 5, or 2 times greater than the approval test. The average value for the two samples was 99 MPa, with 68% higher than the approval test.

4. Conclusions

Crystallization and unidirectional solidification in an aluminum alloy were obtained using a three zone furnace with the solidifying melt placed in a mobile crucible moving vertically upwards. Solidification conditions have been varied based on a set of four melting – solidification – cooling diagrams. Based on these diagrams, 6 samples have been obtained in the Bridgman furnace, one for the approval test and the other 5 at 973 K (700°C), 1023 K (750°C) and 1073 K (800°C) temperatures. These samples were used for mechanical investigations. The approval test had the same value for the compression strength, regardless of the analysis position, respectively zone I or zone II. For the other samples it was noticed that the compression strength was influenced by the increase of the overheating temperature and cooling rate. The highest compressive strength was obtained for the 1073 K (800°C) overheating temperature and was approximately 37% higher than the approval test. Comparing the values of compressive strength for the same sample, but considering the delimitation zone, it was remarked a significant difference, between 10% and 20%. Generally speaking about the solidification in the Bridgman furnace, one can say that the solidification – cooling rate affects in a visible and favorable manner the compressive strength, as a result of the columnar structure formed in the unidirectional solidification.

R E F E R E N C E S

[1]. *C. Batur, W. M. B. Duval, R. J. Bennett*, "Performance of Bridgman furnace operating under projective control", in Proceedings of the 1999 American Control Conference, **vol. 6**, 1999, pp. 4101-4105;

[2]. *M. Margulies, P. Witomski, T. Duffar*, "Optimization of the Bridgman crystal growth process", in Journal of Crystal Growth, **vol. 266**, iss. 1-3, 2004, pp. 175-181;

[3]. ***, Operation and maintenance manual for TvU vacuum/gas tube furnace, Thoughtventions Unlimited LLC PO Box 1310 (40 Nutmeg Lane) Glastonbury, CT 06033;

[4]. *N. Şerban, V. D. Cojocaru, M. Buţu*, "Mechanical behavior and microstructural development of 6063-T1 aluminum alloy processed by equal-channel angular pressing (ECAP): pass number influence", in JOM: Journal of The Minerals, Metals & Materials Society, **vol. 64**, iss. 5, 2012, pp. 607-614;

[5]. *N. Şerban, N. Ghiban, V. D. Cojocaru*, "Mechanical behavior and microstructural development of 6063-T1 aluminum alloy processed by equal-channel angular pressing (ECAP): die channel angle influence", in JOM: Journal of The Minerals, Metals & Materials Society, **vol. 65**, iss. 11, 2013, pp. 1411-1418;

[6]. *V. D. Cojocaru, D. Răducanu, N. Şerban, I. Cincă, R. Şaban*, "Mechanical behaviour comparison between un-processed and ECAP (Equal Channel Angular Pressing) processed 6063-T835 aluminum alloy", U.P.B. Sci. Bull. Series B, **vol. 72**, iss. 3, 2010, pp. 193-202;

[7]. *F. Ştefănescu, G. Neagu, A. Mihai, I. Stan*, "Controlled Temperature Distribution and Heat Transfer Process in the Unidirectional Solidification of Aluminium Alloys", in Solid State Phenomena, **vol. 188**, 2012, pp. 314-317;

[8]. *J. D. Hunt*, Solidification and casting of metals: Proceedings of an international conference on solidification, Book (The Metals Society), **vol. 192**, London, 1979;

[9]. *A. J. Elliott, T. M. Pollock*, "Thermal Analysis of the Bridgman and Liquid-Metal-Cooled Directional Solidification Investment Casting Processes", in Metallurgical and Materials Transactions A, **vol. 38**, iss. 4, 2007, pp. 871-882;

[10]. *A. J. Elliott, G. B. Karney, M. F. X. Gigliotti, T. M. Pollock*, "Issues in Processing by the Liquid-Sn Assisted Directional Solidification Technique", in Superalloys 2004, TMS (The Minerals, Metals & Materials Society), 2004, pp. 421-430;

[11]. *A. Kermanpur, M. Rappaz, N. Varahram, P. Davami*, "Thermal and grain-structure simulation in a land-based turbine blade directionally solidified with the liquid metal cooling process", in Metallurgical and Materials Transactions B, **vol. 31**, iss. 6, 2000, pp. 1293-1304;

[12]. *A. J. Elliott, T. M. Pollock, S. Tin, W. T. King, S. C. Huang, M. F. X. Gigliotti*, "Directional solidification of large superalloy castings with radiation and liquid-metal cooling: A comparative assessment", in Metallurgical and Materials Transactions A, **vol. 35**, iss. 10, 2004, pp. 3221-3231;

[13]. *V. D. Cojocaru, N. Şerban, D. Răducanu, I. Cincă, R. Şaban*, "Microstructural observations of fracture surfaces for a 6063-T1 ECAP processed aluminum alloy", in U.P.B. Sci. Bull. Series B, **vol. 72**, iss. 4, 2010, pp. 163-172;

[14]. *N. Şerban, D. Răducanu, V. D. Cojocaru*, "X-Ray diffraction study and die geometry effect on structural and mechanical characteristics of a nanosized severely deformed 6063 aluminum alloy", in Optoelectronics and Advanced Materials – Rapid Communications, **vol. 9**, iss. 9-10, 2015, pp. 1197-1203;

[15]. *I. Stan*, Researches concerning the metallic materials properties improving by directing solidification, PhD Thesis, University Politehnica of Bucharest, 2015.